Published May, 1973

Soil Concretions: I. X-Ray Spectrograph and Electron Microprobe Analyses[1]

R. N. GALLAHER, H. F. PERKINS, AND D. RADCLIFFE[2]

ABSTRACT

X-ray spectrographic analyses of soil concretions collected in Georgia and Tennessee from different soil parent material and moisture regimes indicated wide variation in chemical composition. Analyses showed higher concentrations of Mn and Ba in the inner core than in the outer layer of Fe-Mn concretions from Henry and Iredell soils. A larger concentration of Fe and Ti was found in the outer layer as compared to the inner core. Distribution of Mn, Ba, Fe, and Ti indicated that they were accumulated by a similar mechanism in Henry and Iredell Fe-Mn concretions. Concretions from the Tifton soil were composed of randomly distributed quartz grains cemented by Fe, Al, and Si oxides; whereas, those from the Decatur soil consisted of a homogenous mixture of Mn and Ba oxides. Electron probe micrographs supported the indication that elemental distribution within concretions differed as a result of weathering conditions at different geographic locations.

Additional Index Words: structural water, Fe-Mn concretions, elemental composition.

CONCRETIONS have been found in many soils. The quantity, chemical composition, and size of concretions in soils depends upon the action of weathering processes for that locale. Murthy and Mathur (10) and Winters (18) concluded that concretions were a mixture of soil material cemented together. According to Murthy and Mathur (10), the cementing agents for Fe-Mn concretions were oxides of Fe and Mn. Iron-Mn concretions contained higher quantities of Mn and Fe than the soils in which they occurred (13, 18). Winters (18) observed that large concretions contained more Mn than small ones, and Murthy and Mathur (10) found that dark colored concretions were high in Mn content.

Conditions favorable for soil concretion formation include poor drainage (3, 14, 16) usually associated with level topography, light colored soils, and Solonetz-like soils (18). A probable mechanism of mottling and concretion formation in poorly drained soils was proposed by Blume (3). He stated that Fe on the aggregate surface became dissolved on reduction and was transported into the interior of the aggregate. If, upon drying, O_2 diffuses into the aggregate and causes precipitation of $Fe(OH)_3$, nodules or mottles formed according to the rate of O_2 diffusion. Blume concluded that mottling was an imperfect formation of concretions.

Large quantities of Mn concretions are found in marine environments (4, 5, 9, 15, 17). Studies on Mn concretion formation in marine environments may aid in understanding the mechanism of Fe-Mn concretion formation in poorly-drained soils. Riley and Sinhaseni (15) found that the hydrochloric acid-insoluble fraction of ocean floor nodules was composed primarily of clay minerals. Lesser quantities of quartz, apatite, biotite, and Na and K feldspars were present. Burns and Fuerstenau (5) studied interelement relationships in Mn nodules using an electron probe microanalyzer. They found that the Fe concentration fluctuated, whereas the Mn concentration was relatively uniform throughout the nodule.

The purpose of this investigation was to compare the chemical composition of concretions developed under different environments in several soil types in Georgia and Tennessee.

MATERIALS AND METHODS

Concretions were collected from the Ap horizon of Henry silt loam and the Ap and B21t horizons of Iredell fine sandy loam (Table 1). Henry soils, which contain a fragipan, are wet most of the year due to a high water table. Iredell soils are wet during winter and early spring and during periods of excessive rainfall. These soils have a relatively impervious argillic horizon. Henry and Iredell concretions are similar in appearance, both being somewhat spherical in shape, and have a strong brown (7.5YR 5/6) and (7.5YR 5/8) surface coating, respectively, encasing a very dark gray (7.5YR 3/0) core. Concretions from both soils were soft, each having a hardness of <2 on Mohs' scale, and ranged in size from <1 mm in diameter to >1 cm. Two other types of concretions were studied. One type was obtained from the Ap horizon of a Tifton loamy sand and the other was collected from the surface of a Decatur loam soil in Bartow County, Georgia (Table 1). No attempt was made to differentiate the layers of these concretions. Tifton concretions had a red to yellowish-red (5YR 4/6) matrix and those from Decatur, a Black (2.5YR 2/0) matrix. Each of these types of concretions had a hardness of 4 or more on Mohs' scale.

X-Ray Spectrograph Analyses

Concretions were washed free of soil material and dried at 100C for 12 hours. Fifteen concretions 6–8 mm in diameter from Henry and Iredell soils were separated into the surface coating (light colored material) and core (dark colored material) by cracking the concretions and scraping the soft core material away from the surface coating with a knife and dissecting needle. The surface coating varied in thickness and averaged approximately 1 mm in most concretions. A specific size of 6–8 mm in diameter was used to avoid possible differences in elemental content due to size as reported by Winters (18). An additional 15 concretions of comparable size from each of the two locations and from the Tifton soil were used for composite analyses of surface and core material. Since the concretions from Decatur soil were fused together, a 7–8 g fragment was used for analysis.

Samples were crushed and dried at 60C overnight. Each sample was ground in a tungsten carbide ball mill to pass a 325-mesh screen (1). A sample was prepared for analysis by pelleting 0.8 g of the concretion with 0.2 g cellulose binder. The pelletized samples were made with a cellulose back and edge for structural strength and designed to fit into Norelco sample holders (11). Standards for Mn, Ba, and Fe were prepared from analytical grade MnO_2, $BaSO_4$, and Fe_2O_3, respectively. Other standards were prepared from minerals of known chemical composition.

[1] Contribution from the Univ. of Georgia, College of Agr. Exp. Sta., College Station, Athens, Ga. 30602. Received Sept. 18, 1972. Approved Feb. 22, 1973.

[2] Graduate Research Assistant, Professor of Agronomy, and Former Assistant Professor of Geology, Univ. of Georgia, Athens. Present address of third author, Senior Geologist, C-E Minerals, 4026 Lexington Rd., Athens, Ga .30601.

Table 1—Source of soil parent material and textural properties of concretions

Name	Soil classification	Location	Residuum	Geographic	Concretion texture
Henry silt loam	Typic Fragiudalfs; Coarse-silty, mixed, thermic	Weakly County, Tennessee	Mixed loess	Deep Loess	Pisolitic
Iredell fine sandy loam	Typic Hapludalfs; Fine, montmorillonitic, thermic	Elbert County, Georgia	Basic igneous rock	Southern Piedmont	Pisolitic and framboidal
Tifton loamy sand	Plinthic Paleudults; Fine-loamy, siliceous, thermic	Tift County, Georgia	Marine sediments underlain by limestone	Southern Coastal Plains	Pisolitic porous
Decatur loam	Rhodic Paleudults; Clayey, kaolinitic, thermic	Bartow County, Georgia	Crystalline rocks	Blue Ridge	Framboidal

Table 2—Operating conditions for the Norelco X-ray spectrograph

Element	X-ray measured	Crystal	X-ray tube	Detector voltage
				kV
Ba	$L_{\alpha 1}$	LiF	Cr	1.7
Fe	$2K_{\alpha 1}$	EDdT*	Mo	1.65
Mn	$K_{\alpha 1}$	LiF	Cr	1.7
Tl	$K_{\alpha 1}$	LiF	Cr	1.7
Ca	$K_{\alpha 1}$	EDdT	Cr	1.7
K	$K_{\alpha 1}$	EDdT	Cr	1.7
Si	$K_{\alpha 1}$	EDdT	Cr	1.8
Al	$K_{\alpha 1}$	EDdT	Cr	1.8

* Ethylene diamine ditartrate.

Calcium, K, Si, Al, Ba, Mn, Fe, and Ti were determined using a full-wave rectified Norelco vacuum X-ray spectrograph. The operating conditions for the spectrograph are given in Table 2. A gas flow proportional detector was used for all elements. First-order $K_{\alpha 1}$ radiation was measured for all elements except for Ba and Fe. Second-order $K_{\alpha 1}$ radiation was selected for Fe because of Mn K_β radiation interference in the samples (1). First order $L_{\alpha 1}$ radiation was used for Ba.

Weight loss was determined by first drying samples at 100C for 1 hour and then heating at 800C for 2 hours in a muffle furnace. Weight loss was the loss in weight between 100 and 800C.

Electron Probe Microanalyzer Analyses

Concretions of sizes similar to those used for X-ray spectrographic analysis were used for microprobe analysis after mounting in a methacrolate monomer according to Gallaher, Perkins, and Radcliffe (6). Samples were coated with a 300–400Å film of carbon in a vacuum evaporator prior to microanalysis in a model MAC 400S instrument. Analysis involved standard electron beam scanning over the desired area of the specimen. Areas up to 300 μ^2 were examined. Backscattered electrons (BSE) and characteristic X-ray scanning images were displayed on a slow phosphor oscilloscope and recorded photographically. The BSE image is sensitive to variation in mean atomic number and displays essentially the variation in phase chemistry. The X-ray images show the relative distribution of individual elements in which semiquantative variations appear as varyng shades of white (high concentration) and black (low concentration). All samples were analyzed with an acceleration voltage of 25 kV. A LiF analyzing crystal was used for the analyses of Ti, Ba, Mn, and Fe, an ammonium dihydrogen phosphate (ADP) crystal for Si and a potassium acid phtallate (KAP) crystal for Al. A gas flow proportional detector was used for Ti, Ba, Al, and Si, and a sealed proportional detector was used for Mn and Fe. Pure metal standards were used for Ti, Mn, Fe, Al, and Si and bentonite ($BaTiSi_3O_9$) for Ba.

RESULTS AND DISCUSSION

X-Ray Spectrograph Chemical Analyses

Results of chemical analyses expressed on the basis of oxide weight percent are shown in Table 3. The bulk of concretions from Henry and Iredell soils were composed primarily of Fe_2O_3, MnO, SiO_2, Al_2O_3, and weight loss components. Concretions from Henry and Iredell soils contained approximately 60 and 100% more BaO and MnO, respectively, in the core than in the surface layers. Composite concretions from Iredell had 30% more BaO and 60% MnO than the Henry concretions (Table 3) and in addition contained considerable quantities of TiO_2. These data indicate that Mn is positively related to concretion color which is in agreement with Murthy and Mathur (10), who found that high Mn content was associated with dark colored material. Further supporting evidence of dark colors associated with Mn is the high content of MnO found in the concretions from the Decatur soil which were uniformly black (Table 3).

Eleven and one-half and 8% more Fe_2O_3 and slightly more TiO_2 was found in the surface layer than in the core of Henry and Iredell concretions, respectively (Table 3). Most other elements appeared to be equally distributed between the surface and core of Henry and Iredell concretions (Table 3). Calcium oxide was almost twice as high in the Iredell as that of the Henry concretions. This is probably due to the basic rock parent material from which Iredell soil is derived. Henry concretions contained approximately 10 times more K_2O than the Iredell. This may be related to the K bearing primary mineral content found in the two soils. Iredell soils are low in K bearing primary minerals (Mr. Arifin, 1971. Relationship of potassium fixation with certain structural properties of clays in selected southern soils of the U. S. M. S. Thesis. University of Georgia, Athens). Iredell concretions contained more Fe_2O_3 and less SiO_2 than the Henry concretions. Aluminum ox-

Table 3—X-ray spectrography analysis of soil concretions in weight percent

	Henry Ap			Iredell Ap			Iredell B21t	Decatur Ap	Tifton Ap
Oxide	Surface	Core	Composite	Surface	Core	Composite	Composite	Composite	Composite
BaO	0.14	0.22	0.19	0.19	0.31	0.25	0.11	14.49	0.02
Fe_2O_3	24.29	20.49	29.69	44.86	41.24	39.54	42.12	0.00	47.81
MnO	4.43	9.45	7.19	7.70	15.06	11.48	9.17	75.60	1.47
TiO_2	1.01	0.93	0.91	5.71	5.33	6.08	4.46	0.16	0.62
CaO	0.64	0.60	0.70	1.15	1.19	1.28	0.77	0.14	0.02
K_2O	1.48	1.49	1.43	0.19	0.16	0.12	0.00	0.09	0.00
SiO_2	60.75	61.26	52.16	27.25	24.53	27.20	27.42	0.99	30.22
Al_2O_3	8.11	8.36	7.65	9.09	8.79	8.82	10.38	2.56	14.63
Weight loss	4.96	4.82	5.56	8.94	8.76	8.62	10.54	4.80	6.29
Total	105.81	107.62	105.68	105.08	105.37	103.39	104.97	98.83	101.08

ide was slightly higher in the Iredell concretions than the Henry.

Some of the weight loss was apparently structural H_2O associated with Fe_2O_3 and Al_2O_3 (Table 3). These oxides and weight loss components were higher in Iredell concretions of the B21t than those in the adjacent Ap horizon. Since smectites are present in these soils, part of the weight loss may be associated with structural H_2O of clay minerals. During concretion formation, soil material is cemented together (10, 18) and concretions in the argillic horizon would have a higher clay mineral content than those in the surface horizon.

The composition of concretions from the Decatur soil, which was primarily MnO and BaO (Table 3), shows that this material is possibly the mineral psilomelane (8). Decatur concretions have compositions (Table 3) comparable to psilomelane from Mexico and California as reported by Hewett and Fleischer (7). The name psilomelane now is used for the Mn mineral in which Ba predominates (2) and is at times found as concretionary masses in clays (2, 12). Decatur concretions appear to be a Mn mineral or ore of which it is obvious that Ba predominates (Table 3) and which occurs as concretionary masses. X-ray diffraction analysis of the Decatur concretions would be required to confirm or deny that they are psilomelane.

The Tifton concretions consisted almost entirely of Fe_2O_3, SiO_2, Al_2O_3, and weight loss material (Table 3). The low MnO content apparently accounts for the lack of dark colored material.

The composition of the Henry, Iredell, and Tifton concretions exceeded 100% when expressed as the oxide (Table 3). This suggests that not all the elements were in the form reported. In most spectrographic analyses, corrections must be made for various chemical effects. None were made in this study as the basic data necessary for corrections is poorly known in this mineralogical system. Adler (1) reported that mean atomic number, absorption, and fluorescence effects must be considered for accurate quantitative analyses. Attempts were made to eliminate or hold these factors to a minimum by choosing or preparing standards of similar composition.

Electron-Probe Microanalyzer Analyses

The authors deemed it necessary to reemphasize procedures used to aid in better understanding of the results of electron probe analysis discussed below. All concretions were studied under a perpendicular incident reflected light microscope prior to microprobe analyses. In some instances, composite concretions were observed consisting of several small concretions cemented together to form larger ones. Microscopic examination of an Iredell concretion, 5–6 mm in diameter, indicated that it was composed of four small concretions cemented together (framboidal).

The electron probe microanalyzer made it possible to analyze material in small areas ($< 5\mu$) on the surface of solid specimens. Electron beam scanning of selected areas of a concretion produced a picture of the relative concentration of a specific element throughout the areas. This permitted interelement relationships to be established. Profiling the X-ray intensity simultaneously enabled variations of element composition to be compared in a given area of the concretion. Phase correlations from electron-probe measurements assisted in obtaining more accurate information concerning bulk chemical analyses.

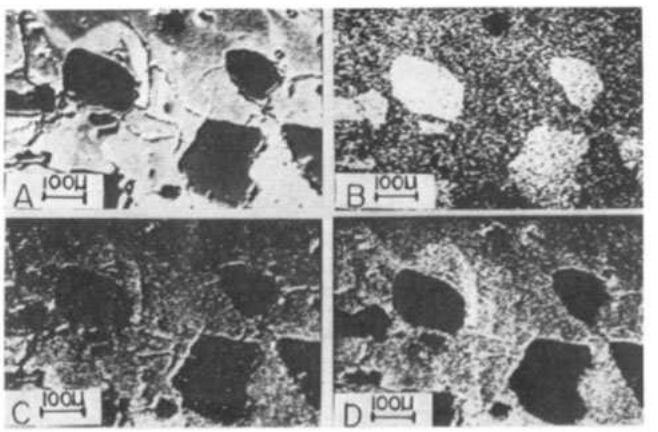

Fig. 1—Electron beam scanning photographs of back-scattered electrons and selected characteristic K_α radiations from a polished section of a Tifton soil concretion. Letter designations refer to: *A*—Back-scattered electrons; *B*—Si K_α X-radiation (light areas); *C*—Al K_α X-radiation (light areas); and *D*—Fe K_α X-radiation (light areas).

Electron beam scanning photographs of an area of a Tifton concretion are shown in Fig. 1. Figure 1*A* is a phosphoroscope display of BSE. The bright areas in the BSE photograph are regions of higher mean atomic number. These areas consist of Si, Fe, and Al which appear to be cementing agents encasing quartz grains that occur as dark areas. The remaining photographs in Fig. 1 are displays of K_α radiation of Si, Al, and Fe distribution over the scanned area. Bright areas are regions of higher element concentration relative to dark areas. The K_α radiation photographs illustrate that the dark areas of the BSE in Fig. 1*A* are quartz and that Si, Al, and Fe are distributed throughout the bright areas. The distribution of Si and Al throughout the matrix (Fig. 1*B* and *C*) indicates the presence of clay minerals. Iron, Al, and Si oxides (Fig. 1), which are distributed throughout the matrix, appear to be the binding material in Tifton soil concretions.

Chemical analysis of minerals with the electron-probe using Fe, Ti, and Si metal standards, showed that ilmenite ($FeTiO_3$) and quartz (SiO_2) minerals were distributed throughout the Iredell concretions. Surrounding these minerals, as was observed by K_α radiation displays, were the elements Si, Al, Ba, Mn, and Fe. Figure 2*A* is a BSE picture of an area of an Iredell concretion. The K_α radiation photographs (Fig. 2*B* and *D*) indicate that the mineral ilmenite is present. This can be verified by comparing the K_α radiation for Ti, Fig. 2*B*, and Fe, Fig. 2*D*, with the light colored minerals in top left and center of Fig. 2*A*. Some of the dark material in Fig. 2*A* is quartz as may be verified by Si K_α radiation in Fig. 2*C*. The light colored material to the right in Fig. 2*A* is a micronodule of Fe encasing numerous small quartz grains as indicated by Si and Fe K_α radiation in Fig. 2*C* and *D*, respectively. Numerous micronodules of Fe were observed in Iredell concre-

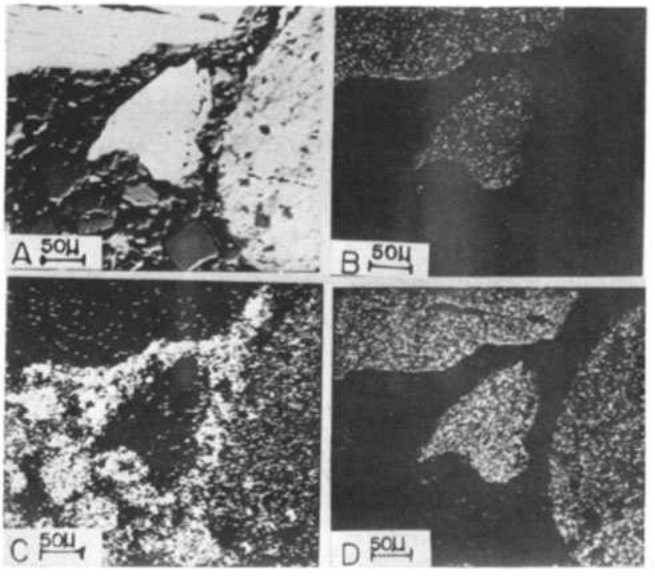

Fig. 2—Electron beam scanning photographs of back-scattered electrons and selected characteristic K_α radiations from a polished section of a Iredell soil concretion. Letter designations refer to: *A*—Back-scattered electrons; *B*—Ti K_α X-radiation (light areas); *C*—Si K_α X-radiation (light areas); and *D*—Fe K_α X-radiation (light areas).

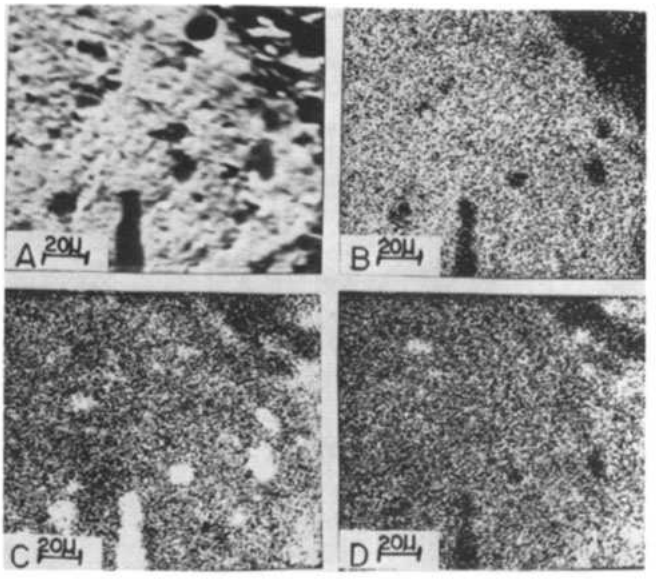

Fig. 3—Electron beam scanning photographs of back-scattered electrons and selected characteristic K_α radiation from a polished section of a micronodule in Iredell soil concretions. Letter designations refer to: *A*—back-scattered electrons; *B*—Fe K_α X-radiation (light areas); *C*—Si K_α X-radiation (light areas); and *D*—Al K_α X-radiation (light areas).

tions. The lack of Fe distribution throughout the matrix of the Iredell concretions (Fig. 2*D*) may account for these concretions being easier to crush than the Tifton concretions in which Fe was distributed throughout the matrix (Fig. 1*D*).

Figure 3 is a larger magnification on the surface of a micronodule in Iredell concretions. The micronodule appears to be an Fe-clay complex encasing quartz grains approximately 10 $\pm$ μ in size. This is based on the phase

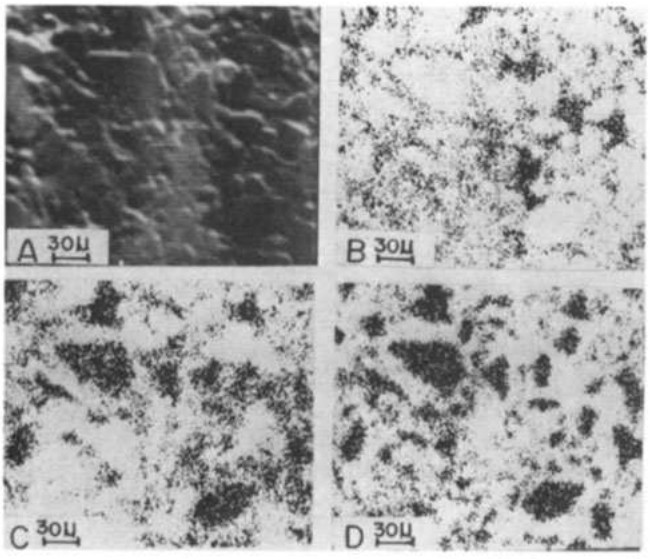

Fig. 4—Electron beam scanning photographs of back-scattered electrons and selected characteristic K_α radiation from a polished section of a Henry soil concretion. Letter designations refer to: *A*—back-scattered electrons; *B*—Si K_α X-radiation (light areas); *C*—Al K_α X-radiation (light areas); and *D*—Fe K_α X-radiation (light areas).

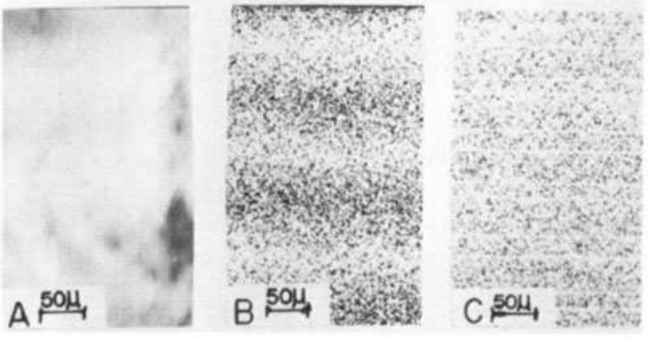

Fig. 5—Electron beam scanning photographs of back-scattered electrons and selected K_α X-radiation from a polished section of a Decatur soil concretion. Letter designations refer to: *A*—back-scattered electrons; *B*—Mn K_α X-radiation (light areas); and *C*—Ba K_α X-radiation (light areas).

chemistry of the BSE image of Fig. 3*A* and the distribution of Fe, Si, and Al in Fig. 3*B*, *C*, and *D*, respectively.

Micronodules of Fe were not observed in Henry concretions. Microscopic examination along with wavelength scanning of K_α radiation showed that numerous small quartz grains were distributed somewhat uniformly within the Henry concretions. Quartz grains are evident from the BSE image as illustrated in Fig. 4*A* and distribution of Si, Al, and Fe in Fig. 4*B*, *C*, and *D*, respectively.

Another mineral about the same size of quartz was found in Henry concretions but in much less quantity than quartz. Blue fluorescence under the electron beam, lack of phase differences in BSE images, and presence of large amounts of K (Table 3) indicate that this mineral may be a feldspar.

Wavelength scanning showed that Mn and Ba were distributed evenly throughout the Decatur concretions (Fig. 5). The close association of Mn and Ba and evidence of a single phase from the BSE image (Fig. 5*A*) gives further evidence that this may be the mineral psilomelane.

ACKNOWLEDGMENTS

Grateful acknowledgments are extended to the Department of Geology, University of Georgia, for the use of laboratory equipment and the National Science Foundation which provided funds for the purchase of the microprobe equipment through Grant No. GA3930 to the third author.

LITERATURE CITED

1. Adler, I. S. 1966. X-ray emission spectrograph in geology. p. 91–153. Elsevier Publishing Co., Amsterdam, London, and New York.
2. Berry, L. G., and Brian Mason. 1959. Mineralogy concepts descriptions determinations. p. 368–369. W. H. Freeman & Co., San Francisco and London.
3. Blume, H. P. 1967. Zum mechanismus der marmorierung und Konkretionsbildung in stauwasser boden. Z. Pflernähr. Bödenk. 119:124–134.
4. Burns, R. G. 1965. Formation of cobalt (III) in the amorphous FeO nH_2O phase of manganese nodules. Nature 205:999.
5. Burns, R. G., and D. W. Fuerstenau. 1966. Electron-probe determination of inter-element relationships in manganese nodules. Amer. Mineral. 51:895–902.
6. Gallaher, R. N., H. F. Perkins, and D. Radcliffe. 1972. Impregnating soil concretions for electron microprobe analysis. Soil Sci. Soc. Amer. Proc. 36:181–182.
7. Hewett, D. F., and Michael Fleischer. 1960. Deposits of the manganese oxides. Econ. Geol. 55:29.
8. Howell, J. V. 1962. Dictionary of geological terms. p. 403. Dolphin Books, Doubleday & Co. Inc., Garden City, New York.
9. Mero, John L. 1962. Ocean-floor manganese nodules. J. Econ. Geol. 57:747–767.
10. Murthy, R. S., and B. S. Mathur. 1964. Special formation in some alluvial soil profiles of the Ganga river plain of Central Uttar Pradesh—their origin, development and significance. Soils Fert. Abst. 31:148.
11. Norrish, K., and B. W. Chappell. 1967. X-ray fluoresence spectrography. p. 204–210. *In:* Zussman, J. (ed.) Physical methods in determinative mineralogy. Academic Press, Inc. New York.
12. Palache, C., H. Berman, and C. Frondel. 1966. The system of mineralogy of J. D. Dana and E. S. Dana. p. 668–670. John Wiley & Sons, Inc., New York.
13. Polteva, R. N., and T. A. Sokolova. 1967. Investigations of concretions from strongly podzolic soil. Soviet Soil Sci. 7:884–893.
14. Raikov, L., and S. Sapundzhiev. 1966. Natural radioactivity and chemical composition of iron manganese concretions in saline and podzolized soils. Soils Fert. Abst. 30: 105.
15. Riley, J. P., and P. Sinhaseni. 1958. Chemical composition of three manganese nodules from the Pacific ocean. J. Marine Res. 17:466–482.
16. Siuta, J., and B. Florkiewicz. 1965. Investigations on the genesis of calcareous concretions. Soils Fert. Abst. 29:371.
17. Willis, J. P., and L. H. Ahrens. 1962. Some investigations on the composition of manganese nodules, with particular reference to certain trace elements. Geochim. et Cosmochim. Acta. 26:751–764.
18. Winters, Eric. 1938. Ferromanganiferous concretions from some podzolic soils. Soil Sci. 46:33–40.